Smaller and Deeper Lesions Increase the Number of Acquired Scan Series in Computed Tomography-guided Lung Biopsy

Conor J. Walsh, PhD, Bishnu H. Sapkota, MBBS,† Mannudeep K. Kalra, MD,* Nevan C. Hanumara, MSME,‡ Bob Liu, PhD,* Jo-Anne O. Shepard, MD,* and Rajiv Gupta, PhD, MD**

Purpose: To determine factors influencing the number of acquired scan series and subsequently the radiation dose and time during computed tomography (CT)-guided lung biopsies.

Materials and Methods: This Health Insurance Portability and Accountability Act-compliant, institutional review board-approved, retrospective study reviewed 50 consecutive procedures. Each procedure was separated into the following steps: trajectory planning, needle placement, needle insertion (extrapulmonary and intrapulmonary), and sampling and follow-up. The number of scan series, time, and radiation dose were calculated for each procedure and its steps. The effects of patient characteristics (age, sex, history of surgery that violated the pleura), procedure characteristics (needle-pleural angle, patient position), and lesion characteristics (size, depth, lobar location) on the number of scan series for the procedure and each step were evaluated using stepwise linear regression. The overall diagnostic accuracy, pneumothorax rate, and chest tube insertion rate were also calculated.

Results: The mean number of total CT scans was 21, the mean effective dose was 14 mSv, and the mean entrance skin dose was 249 mGy. On average, trajectory planning and needle insertion contributed most to the number of scan series (18.5% and 52.9%, respectively). For trajectory planning, a smaller lesion size and shallower needle-pleural angle were associated with an increased number of scans ($R^2 = 0.200$, $P = 0.005$). During needle insertion, smaller lesions were associated with increased scanning ($R^2 = 0.296$, $P < 0.001$), with both smaller and deeper lesions associated with an increased number of scans during the intrapulmonary component ($R^2 = 0.372$, $P < 0.001$). For the entire procedure, smaller lesions were associated with an increased number of scans ($R^2 = 0.12$, $P = 0.01$).

Conclusion: Lesions that are smaller or deeper in the lung result in a higher number of CT scans, resulting in increased radiation dose and procedure time, with most of these performed during the needle insertion step.

Key Words: computed tomography-guided lung biopsy, lesion size, radiation dose, subtask

(*J Thorac Imaging* 2011;26:196–203)

From the *Department of Radiology, Massachusetts General Hospital, Boston; ‡Department of Mechanical Engineering, Massachusetts Institute of Technology, MA; and †Department of Neurology, University of Mississippi Medical Center, MS.

The authors declare no conflicts of interest.

Reprints: Conor J. Walsh, PhD, Department of Mechanical Engineering, Massachusetts Institute of Technology, 77 Massachusetts Avenue, Room 3-470, Cambridge, MA 02139 (e-mail: walshcj@mit.edu).

Computed tomography (CT)-guided lung biopsy, first reported in 1976,[1] is an indispensible procedure for diagnosing several focal lung pathologies, including cancer.[2] The procedure involves incremental insertion of a needle under CT guidance along a planned trajectory to a desired pulmonary target, from which a tissue core, cytologic aspirate, or microbiological material is retrieved for diagnosis, and treatment is planned accordingly. Traditionally, static CT images are used after each adjustment of the needle to guide it to the desired pulmonary target.

The procedure has a reported diagnostic accuracy of 76% to 95%, a mild, self-limiting pneumothorax rate of 20% to 69%, and a severe pneumothorax rate (ie, those that require a thoracostomy tube placement) of 3% to 32%.[3–13] The range in diagnostic accuracy and pneumothorax rate reflects underlying patient comorbidities (eg, emphysema), procedural difficulty (size, depth, location, etc.), and operator experience. The wide variability in the diagnostic accuracy and complication rate for CT-guided lung biopsy has been shown to be based on lesion size,[3–9] depth from the pleural surface,[3,4,6,7] needle-pleural angle,[10] the presence of emphysema,[6,10,11] and the needle gauge.[12]

As discussed, previous literature focuses on the factors that negatively affect diagnostic accuracy and complication rate for CT-guided lung biopsy. However, to the best of our knowledge, there have been no previous studies on correlating number of acquired CT scan series with various patient, procedure, and lesion characteristics. Given the concern over radiation dose associated with CT scanning, it is important to understand the factors that affect its use.

MATERIALS AND METHODS

Study Population

This retrospective study was approved by the institutional review board and complied with the Health Insurance Portability and Accountability Act; informed patient consent was waived. Fifty consecutive patients underwent CT-guided percutaneous lung biopsy at our institution in the 4-month period between September and December 2007. Data analysis was performed by C.J.W. and B.H.S. Of the 50 patients included in our study, there were 26 women and 24 men, with a mean age of 64 years and range of 32 to 89 years.

Biopsy Protocol

All procedures were performed by 1 of 5 board-certified thoracic radiologists with 5 to 26 years of experience in CT-guided lung biopsies. Scanning was

conducted on a 32-channel, multirow detector, helical CT (Somatom Sensation 64, Siemens Medical Solutions, Forchheim, Germany). The patients were instructed to abstain from moving, coughing, talking, or deep breathing during the procedure and the 3-hour postprocedural period.

After reviewing a diagnostic chest CT scan obtained at an earlier date, a single anteroposterior chest localizer scout image was acquired for prescribing the region of interest for scanning. Parameters common to all subsequent scan series included 120 kVp, 0.5-second gantry rotation time, 20×1.2 mm detector configuration (ie, collimated x-ray beam width of 2.4 cm to expose the central 20 detector rows), 1:1 helical pitch, 2.4 mm reconstructed slice thickness, 2.4 mm interslice interval, and medium smooth soft tissue reconstruction kernel (B31f). In all patients, the initial scan series was acquired in a helical mode using the above protocol at a mean effective mAs of 244 (mAs is defined as mAs/pitch), with mAs adjusted based on patient size (range, 168 to 287 mAs). An initial scan of mean length 10.9 cm (range, 5.3 to 25.4 cm) was necessary to localize the suspect lung lesion and plan the procedure. To reduce the radiation dose according to standard department policy, all subsequent scan series were acquired in a sequential or "step and shoot" mode, at a lower effective mAs of 90 to 120, and were limited to a mean length of 2.7 cm (range, 2.4 to 5.3 cm) to cover the region of interest and account for any potential movement between scans.

Procedural sedation with intravenous midazolam (1 to 2 mg) and fenatanyl (50 to 100 μg) was administered in 46 (92%) of 50 patients, sufficient enough to control pain and anxiety of the patient while at the same time aiding consistent, regular, and shallow breathing. The skin was aseptically prepared and draped, and 1% lidocaine (Xylocaine; Astra, Wilmington, DE) was administered locally to induce local anesthesia. A coaxial system composed of a 19-gauge ultrathin introducer needle (Chiba; Cook, Bloomington, IN) and a 22-gauge aspiration needle (Cook) was used to perform the biopsy. Core biopsies, when necessary, were obtained with a 20-gauge cutting needle (Quick-core; Cook).

The procedure was divided into the steps described in Table 1. The first step of the procedure was "trajectory planning." The initial scan series, after the AP scout image, was obtained with a localizing grid (E-Z-EM Fast Find Grid, E-Z-EM Inc., Westbury, NY) placed on the patient to determine the skin insertion point (Fig. 1). This detailed scan showing the grid allows the lesion to be located and any obstructing structures (such as ribs, bullae, and fissures) to be viewed, so as to plan a trajectory that provides a clear path from the skin surface to the lesion. If a clear path to the lesion could not be found from the skin to the lesion due to intervening bony structures and fissures, then the CT gantry was angled in the cranial or caudal direction.

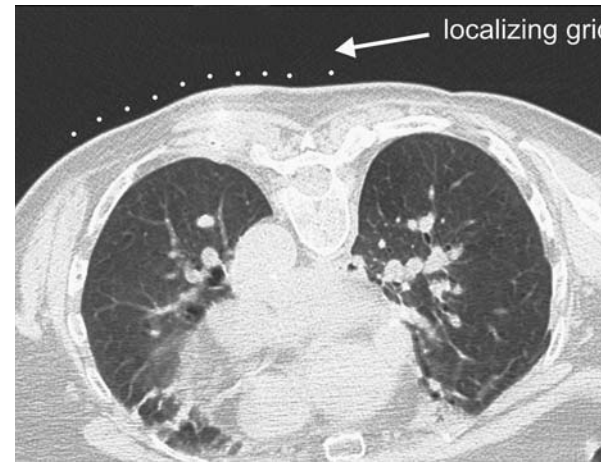

FIGURE 1. A representative CT scan showing both lungs and the localizing grid (arrow) placed over the right lung.

In the next step, "needle placement," after lidocane was injected a small incision was made at the chosen insertion point to facilitate needle entry. A hypodermic needle was left in place as an indicator of the insertion point. Subsequent scanning was performed with necessary positional adjustments to the insertion point, and additional angular adjustments to the gantry were made to ensure that a clear trajectory to the target could be visualized on a single CT slice.

The "needle insertion" step commenced with replacing the indicator needle with the biopsy needle. Needle orientation was typically performed in 2 steps: the needle was first aligned in the craniocaudal direction so that it was in the plane of the gantry. Then, once a confirmatory CT scan showed the needle to be almost completely visible in a single CT slice, the needle was incrementally oriented within the scan plane and advanced, with intermittent CT scanning, to ascertain alignment with the planned trajectory. Typically, most major course corrections were confined to the chest wall. After confirming correct alignment of the needle in the chest wall (extrapulmonary insertion), a single deliberate puncture of the pleura was made, and, once inside the lung, the needle was advanced briskly into the lesion with small angular corrections performed only when absolutely necessary (intrapulmonary insertion).

CT confirmation of the needle in the target indicated the beginning of the "sampling and follow-up" step. The inner stylet of the 19-gauge needle was removed and drops of saline were introduced into the well of the needle to form a water seal to prevent an air embolus entering through the needle and into the bloodstream. The inner 22-gauge aspiration needle was advanced coaxially through the guide needle into the lesion and agitated while suction was

TABLE 1. Four Steps of the Procedure

Procedure Step	Description
Trajectory planning	Determining the desired needle insertion point and skin entry point using a localizing grid
Needle placement	Placing a small hypodermic needle at the desired skin insertion point
Needle insertion	Incremental alignment of needle with desired path and insertion to tumor
Sampling and follow-up	Biopsy sampling and follow-up CT scans between biopsy samples

applied with a syringe. Suction was released before withdrawing the needle so as to not dilute the aspiration sample. The specimen was evaluated by an on-site cytologist, for sample adequacy and volume. Depending on the recommendation of the cytologist, the decision was made whether to obtain additional samples or to perform a core biopsy or microbiology specimens.

Following the removal of the biopsy needles at the termination of the procedure, all patients were positioned puncture site down and monitored closely for 3 hours. Our standard protocol included 1-hour and 3-hour postbiopsy upright chest radiograph in all patients. Patients with small, stable, asymptomatic, postbiopsy pneumothoraces were discharged. A patient with a pneumothorax that was enlarging, or was accompanied by respiratory distress and/or chest pain, required possible chest tube insertion during or after the procedure.

Data Collection

Patient, procedural, and lesion characteristics were obtained from hospital medical records and from a picture archiving and communication system. Age, sex, prior pleural violation, and history of cancer were considered patient characteristics. Procedural characteristics included the position of the patient and the needle-pleural angle. Lesion characteristics encompassed the size of the lesion, its lobar location, distance from the skin to the lesion, distance from the skin to the pleural surface, and distance from the pleural surface to the lesion (Fig. 2). The needle-pleural angle was determined by measuring the angle between a line tangential to the pleural cavity and along the needle length. The number of adjustments to the gantry was determined by counting the number of changes to the angle from the data in the picture archiving and communication system.

A positive biopsy indicating malignancy was considered to be true positive if (1) there was surgical confirmation, (2) the lesion increased in size, (3) other proven metastases were found, or (4) the patient was treated for malignancy and the subsequent clinical course and response to therapy were deemed appropriate. A positive biopsy result was considered to be false positive when there was no evidence of malignancy at surgical resection without preoperative chemotherapy, or when nodule regression in the absence of therapy was documented at follow-up imaging. A negative biopsy result was considered to be true negative when no tumor was identified at histopathologic examination of the surgical specimen, when the lesion subsequently disappeared or decreased in size, or when the lesion remained stable at follow-up CT for 2 years. Negative findings were considered to be false negative if surgical resection yielded a malignant diagnosis or if the lesion increased in size on follow-up.

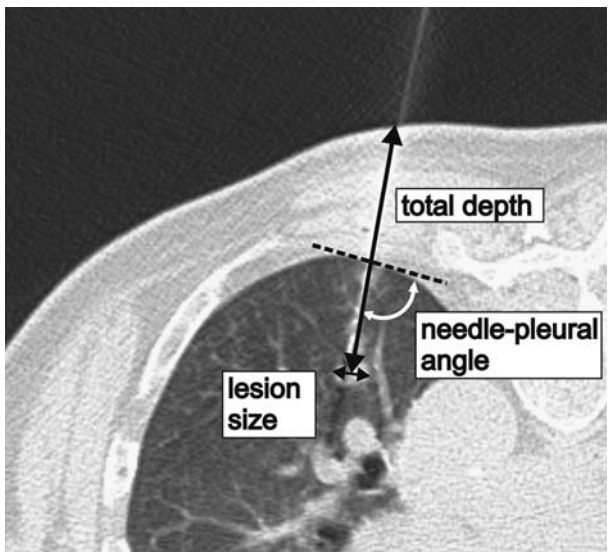

FIGURE 2. A representative CT scan showing the parameters that were recorded from the images.

Radiation Dose and Time

For interventional procedures, the entire ionization effect is concentrated in a few slices (the thorax for the lung biopsy), and therefore it is important to consider both stochastic and deterministic effects of this mode of dose delivery. For the stochastic risk associated with radiation exposure, the dominant notion is that the risk of tumor induction increases linearly with patient dose. The effective dose (E) is used to quantify the stochastic risk, and it takes into account the doses received by all radiosensitive organs weighted according to their radiosensitivity. The entrance skin dose (ESD) is the metric chosen to represent the deterministic dose to the skin of the patient.[13]

E can be derived from the CT dose index (CTDI) values using the ImPACT (Imaging Performance Assessment of CT Scanners) CT Patient Dosimetry Calculator, a Microsoft Excel-based program readily available on the Internet (www.impactscan.org). All scans except for the initial scout scan were included in the dose calculations. The program includes CTDI values normalized per 100 mAs for the center ($CTDI_c$) and periphery ($CTDI_p$) of both body and head phantoms for a wide range of CT scanners and tube potentials. The ImPACT program calculates the weighted CTDI ($CTDI_w$), the volume CTDI ($CTDI_{vol}$), and the dose-length product from the scanning parameters applied in a CT examination. The program then has a mathematical phantom where the region of the patient that was scanned can be defined with the length and location corresponding to the CT bed indicator position. Then, E is determined using the Monte Carlo techniques from coefficients from the National Radiological Protection Board SR250 data sets[14] that are included in the ImPACT program.

The normalized to 100 mAs $CTDI_p$ body phantom values obtained from the ImPACT program were multiplied by the actual mAs values used for the scanning protocol to determine the ESD for each scan. The anatomic location of the maximum ESD_M was calculated by the authors by determining the number of overlapping scans for a procedure and summing their respective ESDs. Thus, a high ESD_M value is due to a repeated scanning of a narrow region of the thorax during an interventional procedure.

The duration of each step, as a portion of the overall procedure, was determined from the CT image timestamps. For each of the steps described above, the number of scan series, E, ESD, step duration, and the number of adjustments to the gantry angle were calculated. The last scan for needle insertion was retrospectively identified when subsequent scans did not evidence any further repositioning of the needle.

Statistical Analysis

The correlations between the number of CT scans and the number of changes to the gantry angle, time, *E*, and ESD were calculated for the total procedure and for each step. The effects of patient characteristics (age, sex, and history of surgery that violated the pleura), procedure characteristics (needle-pleural angle and patient position), and lesion characteristics (size, depth, and lobar location) on the number of scan series were evaluated using univariate and stepwise linear regression. A univariate regression was also performed to determine whether there was a relationship between the number of scans during extrapulmonary and intrapulmonary needle insertion. A strong relationship was deemed to have an R^2 value of 0.49 or higher, a moderate relationship with an R^2 value between 0.09 and 0.49, and a weak relationship with an R^2 value < 0.09. All statistical tests were performed using MedCalc statistical software (MedCalc Software, Mariakerke, Belgium). A P value of < 0.05 was considered to indicate a statistically significant difference.

RESULTS

Patient, Procedure, and Lesion Characteristics

Of the 50 procedures, 35 procedures were performed with the patient in a prone position and the remaining 15 procedures were performed with the patient in a supine position. Conscious sedation was administered in 46 patients, the average needle-pleural angle was 61 ± 16 degrees (range, 34 to 87 degrees), and the average number of changes to the gantry angle was 2.9 ± 2.7. There were 8 patients with surgery that violated the pleural space (eg, partial or full lobectomy) and may have contributed to pleural thickening. Thirty-one patients had a history of cancer, including lung, renal, skin, breast, colon, bladder, ovarian, prostate, and neuroendocrine cancer.

The mean diameter of the lesions was 2.5 ± 1.6 cm (range, 0.7 to 7.9 cm; median, 2.1 cm). The average distance from the skin surface to the lesion was 7.3 ± 2.8 cm (range, 2.7 to 15.2 cm), and the average distance from the costal pleura to the lesion was 2.6 ± 2.3 cm (range, 0 to 7.9 cm). A total of 23 lesions were located in the upper lobes, 4 in the middle lobes, and 23 in the lower lobes. A fine-needle aspiration biopsy was performed in all patients and an additional core biopsy was performed in 7 patients.

Procedure, Radiation Dose, and Time

Overall, there was a large variation in the number of acquired scan series, radiation dose, and procedure time (Table 2). The mean *E* of 14 mSv with CT-guided biopsy was twice that of a typical diagnostic CT examination of the chest[15,16] and 9 (20%) cases had values > 18 mSv.

The mean ESD of 249 mGy was about 10 times that of a typical diagnostic scan. Figure 3 shows a representative CT scan of a biopsy needle placed in a lesion of 0.7 cm in diameter and the corresponding plot of the ESD along the superior-inferior axis of the patient. The peak of the plot represents the anatomic location of the CT image where the needle was scanned multiple times as it was being inserted. The maximum ESD of 534 mGy was observed in a procedure with 38 overlapping scan series, of which 30 covered a 27-mm length of the same anatomic region. The lesion size for this procedure was 1.4 cm.

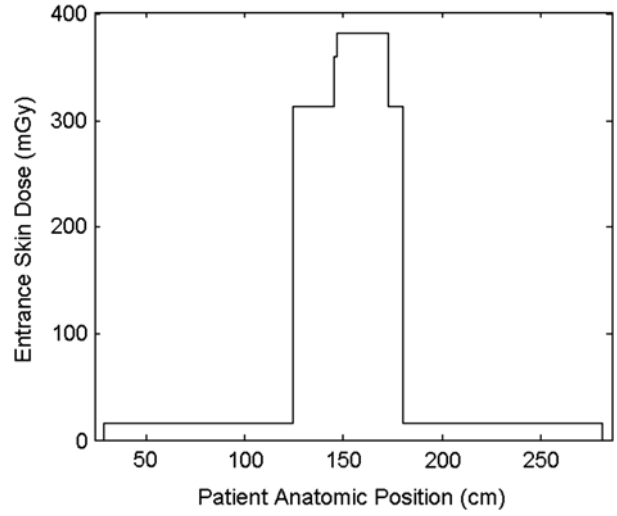

FIGURE 3. Plot of the ESD along the superior-inferior axis of the patient anatomy for a biopsy needle placed in a lesion of 0.7 cm in diameter. In total, 27 scans (13 extrapulmonary and 4 intrapulmonary) were required to place the needle into the lesion with 380 mSv being the value at the peak plateau of this graph.

Procedure Step Analysis

Table 3 shows that, on average, the largest contributor to the average number of scan series was the "needle insertion" step (53%), with 31% and 22% when the needle was extrapulmonary and intrapulmonary, respectively. "Trajectory planning" was the next largest step with a contribution of 19%. The largest contribution to *E* was "trajectory planning" (48%) due to the large length of the first scan. The overall average number of changes to the gantry angle was 2.9 ± 2.7 (range, 0 to 11), with the highest portion (50.4%) occurring during the trajectory planning step.

The average number of CT scans for extrapulmonary and intrapulmonary needle insertion was 6.6 (range, 1 to 16) and 4.5 (range, 1 to 11), respectively. No significant relationship was found between them. The correlations between the number of scans for each step and the time, *E*, ESD, and number of changes to the gantry angle for the respective step are listed in Table 4. For the complete procedure, the number of CT scans performed was strongly

TABLE 2. Summary of Radiation Dose and Procedure Time

	No. Scan Series	ESD (mGy)	*E* (mSv)	DLP (mGy cm)	Time (min)
Range	11-38	126-534	5-34	404-2062	32-121
Median	20	233	13	845	55
Mean ± SD	21 ± 6	249 ± 83	14 ± 6	924 ± 382	59 ± 17

DLP indicates dose-length product.

TABLE 3. Mean Percentage Contribution of Each Step of the Biopsy Procedure to the Number of CT Scan Series, *E*, ESD, and Time

	Needle Placement (%)	Trajectory Planning (%)	Needle Insertion (Extrapulmonary/ Intrapulmonary) (%)	Sampling/Follow-up (%)
Scans	18.5	10.1	53.0 (31.4/21.6)	18.4
ESD	26.7	10.9	47.5 (29.3/18.2)	14.9
E	47.7	7.9	33.2 (20.3/12.9)	11.2
Time	28.5	10.1	39.4 (21.0/18.4)	22.0

The values for extrapulmonary and intrapulmonary steps for needle insertion are also shown.

correlated with the procedure time, ESD, and number of changes to the gantry angle, but not with the *E*. From Table 4 it can also be seen that the number of changes to the gantry angle had a strong correlation with the number of CT scans for trajectory planning and needle placement.

Table 5 lists the results of the univariate analysis. The needle-pleural angle was found to significantly affect the number of scans for trajectory planning and insertion. Lesion size was found to significantly affect the number of scans for needle insertion and intrapulmonary needle insertion. Lesion depth in the lung was found to significantly affect the number of scans for intrapleural needle insertion. Lesion size was the only characteristic to significantly affect the total number of scans. Although the lesion size and patient position did not significantly affect the number of scans for trajectory planning, a trend toward significance was observed.

From stepwise linear regression, we found that a small lesion size was associated with an increase in the number of total scan series ($R^2 = 0.123$, $P = 0.012$). Specifically, we found that smaller lesions and more acute needle-pleural angle were associated with an increased number of scans for planning the needle trajectory; smaller lesions were associated with an increase in the number of scans required to insert the needle along a desired trajectory, and smaller, deeper lesions were associated with an increased number of scans during needle insertion from the pleural surface to the lesion. The factors that significantly affect the number of CT scans for each of the procedure steps are shown in Table 6. The results for a portion of the procedure where the needle is being inserted from the pleural surface to the lesion are also shown and are part of the needle insertion step.

All other patient, procedure, and lesion characteristics were not found to significantly affect the number of scans for any of the procedure steps. Figure 4 plots the number of scans for the needle insertion step as a function of lesion size to illustrate that a significantly higher number of CT scans is required for smaller lesions.

Diagnostic Accuracy and Complication Rate

Of the 50 lesions, 41 diagnosed as malignant and 8 diagnosed as benign were true-positive and true-negative cases, respectively (Table 7), resulting in a diagnostic accuracy of 98%. One case had an inconclusive diagnosis with a failure to exclude metastatic melanoma. A pneumothorax was detected in 12 (24%) patients, 8 (17%) by CT scans during the procedure and 4 (11%) with follow-up chest radiographs. One patient (2%) required thoracostomy for chest tube placement.

DISCUSSION

The lung biopsy procedures included in this study represent a wide spectrum in procedural complexity, and a finding of this study was that more difficult lesions required an increased number of CT scans. We found that on average, the biopsy procedure requires 21 CT scan series and approximately 1-hour elapses between the first and last scan series. These parameters, which are larger than one would intuitively expect, are likely a reflection of our patient population. Being a quaternary care institution, we receive a significant number of referral cases, with a larger proportion of smaller or difficult-to-biopsy lesions. For example, approximately half the lesions included in this study were < 21 mm in diameter.

From Table 3, we can see that insertion of the biopsy needle requires the higher number of CT scans on average, followed by the trajectory planning step. Our analysis showed that the majority of scan series (and hence needle manipulations) were performed when the needle was outside the lung, illustrating the strategy at our institution for minimizing the risk of pneumothorax by having correct needle alignment before puncture of the pleura.

Although the risk of radiation-induced cancer may not be a major concern in the older patient population included in this study, with many patients suffering from primary

TABLE 4. Correlation Coefficients Between the Number of CT Scans and the Number of Changes to the Gantry Angle, time, *E*, and ESD for Each Procedure Step and the Total Procedure Values

Procedural Step	Changes to Gantry Angle (R^2)	Time (R^2)	E (R^2)	ESD (R^2)
Needle placement	0.713	0.816	0.511	0.840
Trajectory planning	0.892	0.359	0.546	0.945
Needle insertion	0.006*	0.588	0.182	0.574
Sampling and follow-up	0.215	0.508	0.383	0.842
Total	0.267	0.495	0.074*	0.573

*Not a significant correlation ($P > 0.05$).

TABLE 5. Results of the Univariate Analysis

	Trajectory Planning	Needle Placement	Needle Insertion	Intrapleural Needle Insertion	Sampling/ Follow-up	Total
Age	0.60	0.54	0.88	0.15	0.96	0.99
Sex	0.46	0.41	0.22	0.46	0.66	0.53
History of surgery that violated the pleura	0.30	0.46	0.26	0.99	0.67	0.50
Needle-pleural angle	0.04*	0.46	0.04*	0.62	0.53	0.55
Patient position	0.07†	0.62	0.59	0.66	0.66	0.96
Lesion size	0.07†	0.92	0.003*	0.002*	0.17	0.01*
Total lesion depth	0.84	0.24	0.32	0.09	0.96	0.70
Lesion depth in lung	0.39	0.17	0.13	0.001*	0.80	0.57
Lesion lobular location	0.13	0.41	0.71	0.20	0.22	0.45

Table lists *P* values between each of the procedure, patient, and lesion characteristics and the number of scans for each of procedure steps and the total number of scans.

*Statistical significance.

†Trending toward significance.

lung cancer or lung metastases, it is nonetheless interesting to understand the factors that lead to increased CT scanning. This study shows that despite the increased scanning for smaller and deeper lesions, the overall mean effective radiation dose was only twice that of a routine chest CT scan. Although increased scanning of the same anatomic location increases the average ESD to about 10 times that of a standard diagnostic chest CT, the average and maximum ESD observed were still below the deterministic threshold for direct radiation-induced damage to the skin. A dose of 2 Gy or higher is required for local skin damage (eg, erythema and epilation).[17,18]

From Table 4, we can see that the number of CT scans was strongly correlated with time and ESD_M. However, the lack of a significant correlation with *E* is due to the significantly higher *E* associated with the long-length initial localizer scan compared with any subsequent shorter scans. Thus, although the number of short-length scans varies significantly with patients, this does not have a large effect on *E*, with the largest contribution coming from the large-length scans for trajectory planning.

All our estimated dose parameters were lower than other theoretical and experimental values reported in the literature for similar CT-guided interventional procedures.[13,19,20] For example, in one case study Tsalafoutas et al[13] reported a maximum ESD_M of 982 mGy from 37 overlapping scans (approximately 26.5 mGy/scan). By comparison, in this study, the ESD_M was 534 mGy from 39 scans (approximately 13.7 mGy/scan). Our low values are in part due to a lowering of the tube current, scan length, and scanning parameters subsequent to the initial localizing scan. We could further reduce the dose by lowering the dose of the very first localizing/planning scan; however, at our institution, the first scan is performed at a normal dose for adequate assessment of perilesional emphysema.

During trajectory planning, there is a significant correlation between the number of scan series and smaller lesion size. This likely reflects the difficulty of determining the correct craniocaudal angulation that aligns the lesion and the skin insertion site, and the task of keeping the biopsy needle coplanar in a single CT slice. Such

TABLE 6. Results From Stepwise Multiple Linear Regression Showing the Factors That Significantly Affect the Number of CT Scans for Each of the Procedure Steps

Procedure Step and Significant Variables	*P*
Trajectory planning	$R^2 = 0.200$, $P = 0.005$
Needle-pleural angle	$P = 0.007$
Lesion size	$P = 0.013$
Needle insertion	$R^2 = 0.207$, $P = 0.003$
Lesion size	$P = 0.003$
Needle insertion (intra-pulmonary only)	$R^2 = 0.312$, $P < 0.001$
Depth in from pleural surface to lesion	$P = 0.005$
Lesion size	$P = 0.009$
Total procedure	$R^2 = 0.12$, $P = 0.01$
Lesion size	$P = 0.01$

All other factors had *P* values > 0.05 and were thus deemed not to be significant and are not included in the table. The R^2 and *P* values for the overall model for each procedure are given along with the individual *P* values for the variables included in the model that were found to be significant.

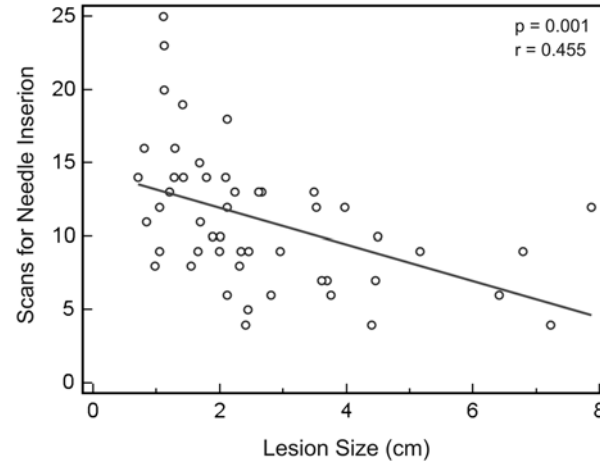

FIGURE 4. Plot of the number of CT scans for needle insertion as a function of lesion size. The *P* and *r* values for a linear regression are also shown.

TABLE 7. Final Diagnoses of Lesions

Malignant Lesions	No. Patients
Bronchogenic carcinoma	
Adenocarcinoma	27
Squamous cell cancer	7
Unclassified carcinoma	3
Metastasis	4
Total	41
Benign lesions	
Infectious processes	4
Inflammation (nonspecific)	4
Total	8

coplanarity makes it easy for the radiologist to plan, visualize, and advance the needle with respect to the target and the surrounding anatomic structures. The strong correlation we found between the number of CT scans and the number of changes to gantry angle during trajectory planning also supports this hypothesis (Table 4). Newer trajectory planning interfaces that facilitate planning across multiple CT slices, with multiplanar reformatting and virtual tilting of the images, can eliminate the need for gantry angle changes altogether.[21]

From Table 4, it is clear that the needle insertion step was the only one that did not have a statistically significant correlation between the number of CT scans and the number of changes to gantry angle. This likely reflects the fact that once a suitable obliquity of the axial plane has been picked during the trajectory planning phase, and the gantry has been tilted to that craniocaudal angulation, most operators work within the chosen scan plane. They compensate for any slight errors by repeated in-plane adjustments of the needle and rescanning. This is reflected in the increased number of scans during this step that is statistically significantly correlated with small lesion size ($P = 0.004$).

Aside from smaller lesion size, a shallower needle-pleural angle also posed a greater challenge during the needle insertion step, as demonstrated by its association with an increased number of CT scans series (Tables 5 and 6). This likely reflects the difficulty of precise needle alignment due to tissue tension, respiratory motion, and limited supporting subcutaneous soft tissue to prevent the needle from falling over. Although shorter biopsy needles (eg, 3 1/2 inch) may be easier to stabilize, they simply cannot be used when accessing lesions deep in the lung. Smaller and deeper lesions also registered increased scanning requirements during the intrapulmonary phase of needle advancement (ie, after the pleural puncture), confirming increased intrapulmonary dwell time and the number of needle manipulations for these lesions.

This highlights the difficulty in targeting small, deeply situated lesions where small angular alignment errors result in large lateral displacements of the distal needle tip because the pivot point for the needle is at the skin surface. Another potential source of error is deflection of the needle due to the reaction force of the tissue acting on the asymmetric beveled tip as the needle is being inserted. These factors affecting needle deflection have previously been highlighted,[22,23] and our results showing that smaller and deeper lesions result in an increased number of scans to advance the needle from the pleural surface to the lesion support this previous work. Although strategies for manually correcting for targeting errors[23] demonstrate promise, new telerobotic systems[24] that align and maintain the needle precisely along an automatically calculated trajectory offer the potential to greatly reduce the difficulty in targeting more challenging lesions.

Retrospective analysis of the practice patterns of the radiologists, as has been done in this study, has its limitations. Such retrospective assessment of radiation dose using the Monte Carlo techniques is an approximation, as it assumes an "average patient" and does not explicitly take actual patient size into account. Furthermore, sequential scan series data only show the aggregate manipulation to the needle from one scan to the next. Although our study accounts for time, radiation dose, and number of CT scans for different steps, it fails to take into account any metrics that have to do with tactile feel or skill of the operator. Being aware of these limitations, this study was specifically designed as retrospective so as to avoid a "Hawthorne effect," where a short-term improvement is caused by the very fact that an operator is being observed or monitored. It should be noted that the technique to angle the gantry so as to have the needle in a single CT slice may not be practiced at other institutions, and thus the radiation dose and time results of this study may not be directly generalizable to other practice settings. Finally, it should be noted that stepwise model selection leads to a bias in those parameters found to be significant because it has searched for the best fit to those specific data. The model that stepwise regression discovers fits better to the data used to discover it than if the model were tested in a new set of data.

The main result of this research, namely that lesions that are smaller and deeper result in a higher number of CT scans and an associated increase in radiation dose and procedure time, highlights the challenge in targeting such lesions in CT-guided procedures. The high diagnostic accuracy and low pneumothorax rate that we found are in line with values from the literature. Additionally, it has long been recognized that accuracy for malignancies is much higher than for benign lesions[25] and with the presence of on-site pathology.[26] Previous studies on CT-guided lung biopsy have not reported the number of CT scans, and with a larger study it would be interesting to examine whether there is a causal relationship between increased perseverance in needle placement (as measured by the number of CT scans in a retrospective study or actual needle manipulations in a prospective study) and high diagnostic accuracy for smaller lesions. Ultimately, the results of this study illustrate the iterative nature of CT-guided interventions. This information highlights the need for hospitals to set low tube current and voltage levels for their CT-guided intervention protocols to minimize the radiation dose per scan, and also to explore the use of devices to aid needle placement to reduce the overall number of CT scans required.

ACKNOWLEDGMENTS

The authors thank the Center for Integration of Medicine and Innovative Technology (CIMIT) for supporting this study. They also acknowledge Dr Eric Macklin for his guidance with the statistical analysis, Dr Ammar Sarwar for his assistance with data collection, and Professor Alexander Slocum for his valuable feedback.

REFERENCES

1. Haaga JR, Alfidi RJ. Precise biopsy localization by computer tomography. *Radiology*. 1976;118:603–607.
2. Manhire A, Charig M, Clelland C, et al. Guidelines for radiologically guided lung biopsy. *Thorax*. 2003;58:920–936.
3. Gupta S, Krishnamurthy S, Broemeling LD, et al. Small (≤2-cm) subpleural pulmonary lesions: short- versus long-needle-path CT-guided biopsy—comparison of diagnostic yields and complications. *Radiology*. 2005;234:631–637.
4. Kazerooni EA, Lim FT, Mikhail A, et al. Risk of pneumothorax in CT-guided transthoracic needle aspiration biopsy of the lung. *Radiology*. 1996;198:371–375.
5. Larscheid RC, Thorpe PE, Scott WJ. Percutaneous transthoracic needle aspiration biopsy: a comprehensive review of its current role in the diagnosis and treatment of lung tumors. *Chest*. 1998;114:704–709.
6. Laurent F, Michel P, Latrabe V, et al. Pneumothoraces and chest tube placement after CT-guided transthoracic lung biopsy using a coaxial technique: incidence and risk factors. *Am J Roentgenol*. 1999;172:1049–1053.
7. Ohno Y, Hatabu H, Takenaka D, et al. CT-guided transthoracic needle aspiration biopsy of small (≤20 mm) solitary pulmonary nodules. *Am J Roentgenol*. 2003;180:1665–1669.
8. Tsukada H, Satou T, Iwashima A, et al. Diagnostic accuracy of CT-guided automated needle biopsy of lung nodules. *Am J Roentgenol*. 2000;175:239–243.
9. Wallace MJ, Krishnamurthy S, Broemeling LD, et al. CT-guided percutaneous fine-needle aspiration biopsy of small (≤1-cm) pulmonary lesions. *Radiology*. 2002;225:823–828.
10. Ko JP, Shepard J-AO, Drucker EA, et al. Factors influencing pneumothorax rate at lung biopsy: are dwell time and angle of pleural puncture contributing factors? *Radiology*. 2001;218:491–496.
11. Cox JE, Chiles C, McManus CM, et al. Transthoracic needle aspiration biopsy: variables that affect risk of pneumothorax. *Radiology*. 1999;212:165–168.
12. Geraghty PR, Kee ST, McFarlane G, et al. CT-guided transthoracic needle aspiration biopsy of pulmonary nodules: needle size and pneumothorax rate. *Radiology*. 2003;229:475–481.
13. Tsalafoutas IA, Tsapaki V, Triantopoulou C, et al. CT-guided interventional procedures without ct fluoroscopy assistance: patient effective dose and absorbed dose considerations. *Am J Roentgenol*. 2007;188:1479–1484.
14. Jones DG, Shrimpton PC. Survey of CT practice in the UK. Part 3: normalised organ doses calculated using Monte Carlo techniques. National Radiation Protection Board, NRPB-R250, Chilton, UK; 1991.
15. Bauhs JA, Vrieze TJ, Primak AN, et al. CT dosimetry: comparison of measurement techniques and devices. *Radiographics*. 2008;28:245–253.
16. Shrimpton PC, Hiller MC, Lewis MA, et al. *Doses From Computed Tomography (CT) Examinations in the UK-2003: Review. NRPB-W67*. Chilton, UK: National Radiological Protection Board; 2005.
17. Geleijns J, Wondergem J. X-ray imaging and the skin: radiation biology, patient dosimetry and observed effects. *Radiat Prot Dosimetry*. 2005;114:121–125.
18. Valentin J. Avoidance of radiation injuries from medical interventional procedures, ICRP Publication 85 [abstract]. *Ann ICRP*. 2000;30:7.
19. Teeuwisse WM, Geleijns J, Broerse JJ, et al. Patient and staff dose during CT guided biopsy, drainage and coagulation. *Br J Radiol*. 2001;74:720–726.
20. Tsapaki V, Triantopoulou C, Maniatis P, et al. Patient skin dose assessment during CT-guided interventional procedures. *Radiat Prot Dosimetry*. 2008;129:29–31.
21. Seitel A, Walsh CJ, Hanumara NC, et al. *Development and Evaluation of a New Image-based User Interface for Robot-assisted Needle Placements With the Robopsy System. Medical Imaging 2009: Visualization, Image-guided Procedures, and Modeling*. Lake Buena Vista, FL: SPIE; 2009: 72610X–772619.
22. Abolhassani N, Patel R, Moallem M. Needle insertion into soft tissue: a survey. *Med Eng Phys*. 2007;29:413–431.
23. Yankelevitz DF, Davis SD, Chiarella D, et al. Needle-tip repositioning during computed-tomography-guided transthoracic needle aspiration biopsy of small deep pulmonary lesions: minor adjustments make a big difference. *J Thorac Imaging*. 1996;11:279–282.
24. Walsh CJ, Hanumara NC, Slocum AH, et al. A patient-mounted, telerobotic tool for CT-guided percutaneous interventions. *J Med Devices*. 2008;2:011007–011010.
25. Khouri N, Stitik F, Erozan Y, et al. Transthoracic needle aspiration biopsy of benign and malignant lung lesions. *Am J Roentgenol*. 1985;144:281–288.
26. Kucuk CU, Yilmaz A, Yilmaz A, et al. Computed tomography-guided transthoracic fine-needle aspiration in diagnosis of lung cancer: a comparison of single-pass needle and multiple-pass coaxial needle systems and the value of immediate cytological assessment. *Respirology*. 2004;9:392–396.